Electrochimica Acta, Vol. 33, No. 11, pp. 1645–1651, 1988.
Printed in Great Britain.

0013–4686/88 $3.00 + 0.00

CHANGES IN THE COMPOSITION OF THE PASSIVE LAYER AND PITTING CORROSION OF STAINLESS STEEL IN PHOSPHATE–BORATE BUFFER CONTAINING CHLORIDE IONS

M. URRETABIZKAYA,* C. D. PALLOTTA,* N. DE CRISTOFARO,† R. C. SALVAREZZA‡ and A. J. ARVIA‡

*Departamento de Fisicoquímica, Facultad de Ciencias Exactas y Naturales, Universidad de Buenos Aires, Argentina
†Departamento de Electroquímica, Instituto Nacional de Technología Industrial (INTI), Argentina
‡Instituto de Investigaciones Fisicoquímicas Teóricas y Aplicadas (INIFTA), Facultad de Ciencias Exactas, Universidad Nacional de La Plata, Casilla de Correo 16, Sucursal 4, (1900) La Plata, Argentina

(*Received* 18 *January* 1988; *in revised form* 19 *April* 1988)

Abstract—The influence of the passive layer properties on the pitting corrosion of 316SS was studied in phosphate–borate buffer containing chloride ions by using potential step and potentiodynamic techniques complemented with scanning electron microscopy. The increase of the anodization time in the passive region decreases the nucleation rate and the mean number of corrosion pits formed on the 316SS surface. Results are explained through changes in the structure and composition of the passive layer during anodization. Two different Cr(III) species can be voltammetrically detected at short anodization times, an outer weakly bound Cr(III) species which is electrooxidized to soluble CrO_4^{2-} and an inner Cr(III) species which is electrooxidized to Cr(VI) but retained in the film at potentials lying in the transpassive region. As the anodization time in the passive region increases, the weakly bound Cr(III) species is transformed into another more stable one, probably an iron chromite, which exhibits an electrooxidation potential more positive than that of Cr(III) species. The aged passive layer becomes more resistant to pit initiation, due to either a decrease in the density of active sites or a decrease in the nucleation rate constant for pit initiation.

INTRODUCTION

The electronic and electrochemical properties of passivating layers play an outstanding role in determining the corrosion resistance of metals and alloys to aggressive environments. The corrosion resistance of those layers is extremely sensitive to their chemical composition. This is the case, for instance, of the influence of alloying elements such as chromium to passive layers of 316 stainless steel (316SS) as far as pitting corrosion is concerned[1, 2].

A typical stabilized voltammogram of 316SS in slightly alkaline buffered solutions (Fig. 1a) shows up three anodic (AI, AII, AIII) and three cathodic current peaks (CI, CII, CIII)[3, 4]. Peak AI was assigned to the electroformation of a $Fe(OH)_2$ layer on the passivating Cr(III) containing layer, peak AII was related to the electrooxidation of the $Fe(OH)_2$ layer constituent to FeOOH, and peak AIII was associated to the electrooxidation of Cr(III) present in the passive layer to Cr(VI) and simultaneous electroformation of soluble CrO_4^{2-} [3]. Correspondingly, peak CIII was related to the electroreduction of Cr(VI) to Cr(III) in the passive layer, peak CII was assigned to the electroreduction of FeOOH to Fe(II), and peak CI was associated to the electroreduction of Fe(II) species to Fe.

At potential values (E) lying within the passive region of 316SS, that is at E values lower than that of peak III, Fe(II)/Fe(III) hydrous oxide layer on a preexisting Cr_2O_3 [3] layer is formed on the metal surface[5], and by increasing the anodization time (t_a), an intermediate layer of a spinel type structure is formed, as concluded recently from XPS data[6]. Furthermore, the dielectric properties of the thin passivating layer, as resulting from high frequency capacitance measurements in the same potential region, depends on the potential sweep rate (v) at which the thin layer was formed ($0.1\ mV\ s^{-1} < v < 2\ mV\ s^{-1}$) that is the history of the passivating layer determines its degree of structural perfection[7].

On the other hand, in chloride ion containing solutions, when the concentration of the aggressive anion exceeds a certain critical value and the applied potential is greater than the breakdown potential (E_b) of the system, the potential–current profiles exhibit a remarkable current increase due to the localized attack of the metal surface (Fig. 1b). The dynamics of this process implies current bursts related to pit activation (birth) and pit repassivation (death) already at potential preceding E_b[7] and also during pit growth[8]. The scattering of pitting parameters such as E_b and induction times (t_i) resulting in early observations was attributed to a lack of control of the experimental conditions, but later it was demonstrated that pitting parameters from rigorously controlled experiments are actually of statistical nature[9]. Similar conclusions can be arrived at from the analysis of the current transients resulting from specimens previously subjected to polarization in the passive region during the time t_a, and later potential stepped to a value E_s greater than E_b. In this case both the potential and time windows determine the type of low governing pitting

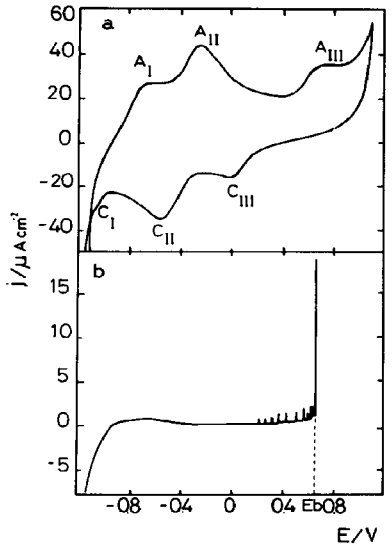

Fig. 1. (a) Stabilized j–E profile of 316SS in phosphate–borate buffer at $v = 0.05\ V\ s^{-1}$ between $E_{s,c} = -1.16$ V and $E_{s,a} = 1.1$ V; (b) j–E profile single recorded at $v = 0.0001\ V\ s^{-1}$ in the phosphate borate buffer containing 0.5 M NaCl. E_b = breakdown potential.

kinetics[10]. Thus, for only a small number of pits, that is E_s slightly more positive than E_b, the kinetics of pitting can be accounted for in terms of a stochastic law[8], whereas for a sufficiently large number of pits, namely $E_s \gg E_b$, a deterministic law is satisfactorily fulfilled[10].

Pitting stability of 316SS specimens appear to be determined by the contents of both Cr(III) and water in the passive layer[11]. The contents of these species can be modified just by changing the applied potential and the temperature. Thus, when the applied potential exceeds the potential of peak AIII a loss of Cr(III) in the passive layer is produced which reduces the ability of the film to self-repair. Otherwise, when the temperature is increased two opposite effects are observed, namely the depletion of Cr(III) in the passive layer hindering repassivation and the formation of a more crystalline passive layer which in turn exhibits a greater resistance to pit initiation.

The present paper emphasizes the influence of the composition and structure of the passive layer on the pitting corrosion behaviour of 316SS in phosphate–borate buffer containing sodium chloride. The changes in composition and structure are brought about by passivation of 316SS specimens at a constant potential for different anodization times (t_a). Subsequently, the electrochemical response is followed either voltammetrically or through potential step measurements. Then, drastic changes in the pitting parameters and in the current–potential profiles are observed. These changes depend on t_a in a very remarkable way as one should expect for a system where the passive layer properties play a determining role on its pitting susceptibility.

EXPERIMENTAL

Specimens cut out from 316SS cold worked rods were axially embedded in Araldite holders to obtain circular exposed working electrodes of about 0.2 cm^2 geometric area. The composition of samples of 316SS rods was the following one in g/100 g: C, 0.05; Mn, 1.00; P, 0.031; S, 0.008; Si, 0.45; Cr, 16.0; Mo, 2.44; Ni, 12.7. Firstly, the metal surface was mechanically polished with fine grained emery paper followed with alumina paste (1 μm dia.) on polishing cloth to obtain a mirror surface. Each polished specimen was rinsed with twice distilled water and dried in air at room temperature. A new pretreated specimen was used for each run. Measurements were made at 25°C with a conventional Pyrex glass cell containing the electrolyte solution (0.2 dm^3). The potential of the working electrode was measured against a saturated calomel electrode (*sce*) provided with a Luggin–Haber capillary tip. All potentials in the text are referred to the *sce*. The electrolyte prepared from AR chemicals and bidistilled water consisted of 0.10 M KH_2PO_4 + 0.05 M $Na_2B_7O_4$ pH = 8 containing 0.5 M NaCl. Previously to each run the solution was purged with purified nitrogen during 3 h. Voltammograms plotted as apparent current density (j) *vs* potential (E), were run by applying to the specimen a singular triangular potential sweep (STPS) between the cathodic ($E_{s,c}$) and the anodic ($E_{s,a}$) switching potentials at different scan rates (v). Potentiostatic current transients were recorded after applying to the specimen a potential program which included successively a cathodization at $E_c = -1.10$ V for 90 s to electroreduce the metal surface, an anodization at $E_a = -0.10$ V for different t_a to form a passive layer, and finally, a potential step to $E_s = 0.60$ V ($E_s > E_b$)[10].

The current transient resulting from each potential step was recorded up to $t_s = 300$ s. The appearance of pitting was detected as a sudden increase in current, once the induction time (t_i) was exceeded. Therefore, to take the real constant pitting time ($t_p = t_s - t_i$) which is required for pit density measurements, t_p was set equal to 40 s. For each t_a 30–40 measurements were made. Due to the ambiguity to define t_i by setting an arbitrary threshold current value to be exceeded, only t_i values for stable pit growth were considered. These values were taken as the last time at which the current was as low as that recorded for the completely passive specimen. This means that for any time, t_s, greater than t_i, the specimen is not able to repassivate. Microscopic observations were made by using a Philips 500 electron scanning microscope.

RESULTS

Current transients obtained by stepping the potential from -0.1 V to $E_s = 0.6$ V by setting t_a values in the $90 < t_a < 3600$ s range were recorded. The current transients change according to t_a (Fig. 2). Thus, for $t_a = 90$ s, they exhibit an initial current decrease, and when the value of t_i is exceeded, the sudden rise in current is related to the nucleation and growth of a large number of pits (Fig. 2a). As t_a increases from 90 s to 900 s, a considerable increase in t_i can be observed (Fig. 2b). This result is accompanied by the decrease of

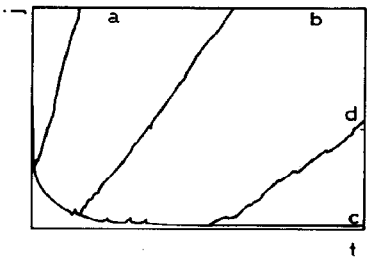

Fig. 2. Schematic representation of the type of current transients run at $E_s = 0.60$ V for 316SS in phosphate–borate buffer + 0.5 M NaCl, after anodization at $E_a = -0.1$ V for different t_a values: (a) 90; (b) 900; (c) 3600; (d) 3600 s. Before prepassivation at E_a the electrodes were cathodized at $E_c = -1.20$ V for $t_c = 90$ s.

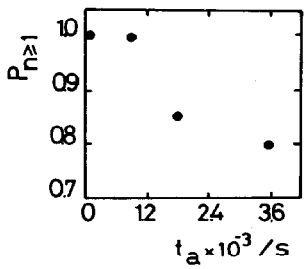

Fig. 3. $P_{n\geq1}$ *vs* t_a plot.

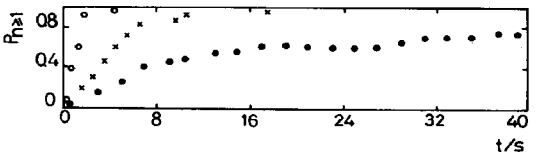

Fig. 4. $P_{n\geq1}$ *vs* t plots (o) $t_a = 90$ s; (x) $t_a = 900$ s; (o) $t_a = 1800$ s.

both the slope of the transient and the number of pits formed on the metal surface. For longer passivation times ($t_a = 3600$ s) a certain number of specimens (20%) exhibit only decreasing transients with a few current oscillations. In these cases the metal surface remained passive and free of pitting attack during the experiment (Fig. 2c). The other 80% developed pitting attack with t_i values longer than those observed for $t_a = 900$ s (Fig. 2d). From the current transients the probability to form at least one single stable pit ($P_{n\geq1}$) for different t_a values, can be calculated (Fig. 3). The increase in t_a results in the decrease of $P_{n\geq1}$, so that for $t_a = 3600$ s, $P_{n\geq1} \to 0.8$. Therefore, the probability of having pitting-free specimens increases according to t_a. For $t_a = 90$ s, practically all specimens undergo pitting before 2 s (Fig. 4). Conversely, for $t_a = 1800$ s only 10% of the specimens develop pitting in the 0–2 s range. Accordingly, the mean number $\langle n \rangle$ of large pits formed for $t_p = 40$ s decreases drastically on increasing t_a (Table 1).

Table 1. Mean number of large pits $\langle n \rangle$ formed at $E_s = 0.60$ V, after passivation at $E_a = -0.1$ V for different t_a, and the corresponding standard deviation (σ)

t_a/s	$\langle n \rangle$	σ
90	30	22
900	7.93	5.18
1800	4	4

The j–E profiles at $v = 1 \times 10^{-3}$ V s^{-1} between $E_{s,c} = -0.1$ V and $E_{s,a} = 0.6$ V were obtained after anodization at $E_a = -0.1$ V for different t_a (Fig. 5). When $t_a = 60$ s, the j–E profile shows up a large number of current oscillations in the entire potential range which are related to the birth and death of pits. These oscillations increase in frequency and amplitude as the applied potential continuously moves along positive direction. Conversely, for $t_a = 3600$ s, the j–E profile remains free of oscillations up to 0.31 V. As the applied potential shifts in the positive direction current bursts are also observed although their number and amplitude are smaller than those resulting for $t_a = 60$ s. Therefore, the background current is also markedly reduced when t_a changes from 60 to 3600 s indicating that the passive layer turns out to be more protective. It can be also noticed that for $t_a = 60$ s, specimens exhibit a large number of birth and death events before the irreversible passive layer breakdown (stable pitting) is attained, whereas for $t_a = 3600$ s irreversible pitting occurs just after only a small number of oscillations. From these results it can be concluded that the increase in t_a definitely enhances the resistance of 316SS to pit initiation, although it also hinders the ability of the film to self-repair. This explanation implies either the

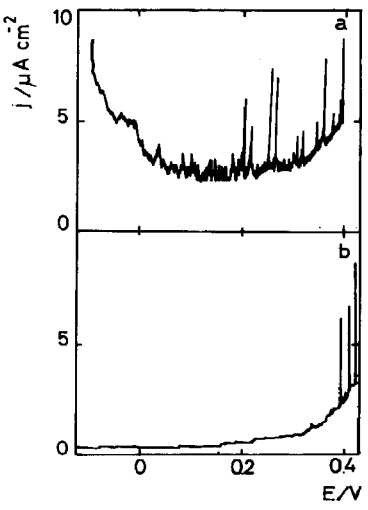

Fig. 5. j–E profiles of 316 SS in phosphate–borate buffer 0.5 M NaCl run at $v = 0.001$ V s^{-1} between $E_a = -0.1$ V and $E_{s,a} = 0.42$ V after anodization at -0.1 V: (a) $t_a = 90$ s; (b) $t_a = 3600$ s.

formation of a thicker passivating layer or structural changes at the passive layer, or both effects acting simultaneously for older passive layers.

The characteristics of the passive layer were further studied through the dependence of t_a on the potential and voltammetric charge density of peaks CII and AIII. Peak CII provides information about the amount and type of Fe(III) species as constituent of the passive layer, whereas peak AIII furnishes additional data about the amount and type of Cr(III) species. After anodization at $E_a = -0.1$ V in the plain buffer, for different t_a, the cathodic j–E profiles covering from $E_{s,a} = -0.1$ V to $E_{s,c} = -1.3$ V at $v = 0.05$ V s^{-1}, shows up no appreciable "ageing" effects as the potential of peak CII remains practically constant for any t_a value in the range covered by the present work. On the other hand, q_{CII}, the voltammetric charge density of peak CII, increases substantially in the early stages of the anodic layer growth, but it reaches a constant value close to 300 μC cm^{-2} when t_a exceeds 60 s (Fig. 6). Similar experiments run in the buffer solution containing 0.5 M NaCl, also involve an initial sharp increase in q_{CII}, and later a linear increase of q_{CII} with t_a. For $t_a = 3600$ s the value of q_{CII} is close to 450 μC cm^{-2} and, in this case, the current calculated from the slope of the q_{CII} *vs* t_a plot is 60 nA cm^{-2}.

Voltammetric runs recorded in the plain buffer solution (first scan) provide further information on the type and amount of the Cr species which is present in the passive layer. These voltammograms were obtained after the specimen was held at $E_c = -1.2$ V for $t_c = 90$ s, later stepped to $E_a = -0.1$ V for $t_a = 90$ s, subsequently ramped to $E_{s,a} = 1.1$ V at $v = 0.05$ V s^{-1}, and finally swept back to $E_{s,c} = -1.2$ V. The corresponding j–E profiles show up in the positive scan covering the transpassive region, two contributions, AIII′ and AIII, located at 0.35 V and 0.80 V, respectively (Fig. 7). It should be noticed that peak AIII′ which appears during the first voltammetric scan can be hardly observed in the stabilized voltammogram resulting after repetitive potential cycling (Fig. 1a). Otherwise, during the negative going potential excursion, peaks CIII and CII show up in the potential range preceding the threshold potential of the hydrogen evolution reaction (HER). Likewise, when $E_{s,a}$ is changed stepwise in the positive direction a net increase in charge of peaks CIII and CII can be observed, whereas the threshold potential of the HER turns out to be more negative. Otherwise, for $E_{s,a}$

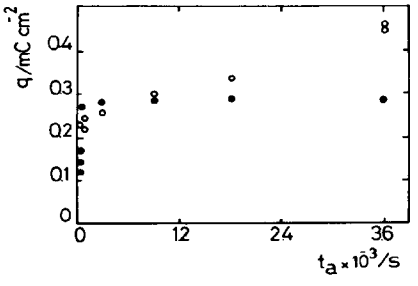

Fig. 6. q_{CII} *vs* t_a plots (o) phosphate–borate buffer; (●) phosphate–borate buffer + 0.5 M NaCl.

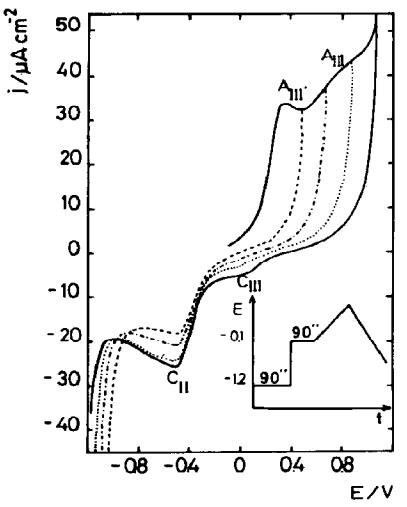

Fig. 7. j–E profiles of 316 SS in phosphate–borate buffer run at 0.05 V s^{-1} between $E_a = -0.1$ V to $E_{s,a}$ stepwise changed in the anodic direction and downwards to $E_{s,c} = -1.20$ V.

$< E_{AIII}$, peak CIII is not longer observed. The behaviour of complementary peaks AIII and CIII seems to be exclusively associated with the Cr(III)/Cr(VI) redox couple in the passive layer. Conversely, peak AIII′ appears to be related to the electrooxidation of Cr(III) to soluble CrO_4^{2-}.

From the dependence of q_{CII} on $E_{s,a}$, it can be also concluded that the electrooxidation of Cr(III) to Cr(VI) occurs simultaneously with the incorporation of Fe(III) into the passive layer. Otherwise, the proper behaviour of the HER already described suggests that the relatively small amount of Fe(II) species remaining at the metal surface increases according to $E_{s,a}$ and t_a. This explains the reason why peak CI (Fig. 1) can be hardly observed along the first voltammetric scan. Similar runs involving the increase in t_a from 90 s to 3600 s (Fig. 8), show up that peak AIII′ moves in the positive direction overlapping peak AIII as t_a increases, although the overall charge density up to 0.60 V remains practically constant (Fig. 9). These results indicate that the electrooxidation of Cr(III) to soluble CrO_4^{2-} is hindered gradually as t_a increases. Furthermore, the potential of peak CIII becomes independent of t_a, although its charge slightly increases with t_a. The addition of NaCl to the buffer in the concentration range where pitting corrosion can be avoided ($c_{NaCl} < 0.05$ M), results in the increase of height of peak AIII and the increase in charge q_{AIII}, in the short time range of t_a, that is for $t_a < 90$ s (Fig. 9).

DISCUSSION

The present results show the outstanding importance of the passive layer properties in determining the pitting behaviour of 316SS specimens in phosphate–borate buffer containing chloride ions. In order to explain the behaviour of this system, let us first

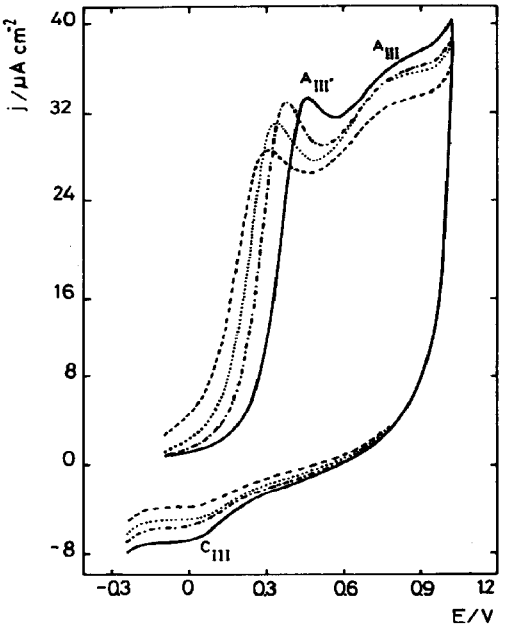

Fig. 8. j–E profiles of 316 SS in phosphate-borate buffer run at 0.05 V s^{-1} between $E_a = -0.1$ V and $E_{s,a} = 1.1$ V and downwards to $E_{s,c} = -0.25$ V after anodization at E_a for different t_a: (– – –) 90; (· · ·) 900, (– · –) 1800; (——) 3600 s.

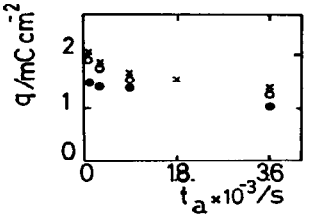

Fig. 9. Plots of the overall charge density (q) of peaks AIII'–AIII (q) *vs* t_a for different c_{NaCl}; (. . .) 0; (ooo) 10^{-2}; (xxx) 5×10^{-2} M.

consider the structure and thickening of the passive film. According to a previous study[5] at $E_a = -0.1$ V, the passive layer approaches a duplex structure consisting of an inner rich C(III) layer and an outer rich Fe(III)/Fe(II) layer containing some Cr(III) species. The fact that the overall charge related to reactions at the inner layer (peak AIII) remains constant up to 0.6 V, indicates that the thickness of this layer is practically constant and independent of t_a. The opposite is, however, found for the charge related to the outer layer. Thus, in the first seconds of the anodization process large changes in film thickness take place as seen from Fig. 6, whereas for $t_a > 60$ s either a practically constant thickness is approached in the buffer solution, or it increases slightly with t_a in the buffer + 0.5 M NaCl solution. For the latter the value of q_{CII} increases from 300 to 450 μC cm^{-2} after 60 min anodization. The change in the thickness of the passive layer (h) can be roughly evaluated from the relationship:

$$h = Mq_{CII}/zF\rho. \quad (1)$$

Let us assume that the outer layer mainly consists of FeOOH species[12, 13], then $M = 88$ g mol^{-1}, $z = 1$ and $\rho = 3.00$ g cm^{-3}. From the values of q_{CII} one obtains values of h ranging from 6.6 Å for $t_a = 60$ s to 13.5 Å for $t_a = 3600$ s. It should also be noticed that a change in t_a from 90 to 900 s, only reflects in the increase of h from 6.6 to 8.4 Å. This difference in h appears to be extremely small to account for the remarkable changes of the pitting corrosion parameters of 316SS specimens. Therefore, a more reasonable explanation of these facts must be sought through changes in the structure and/or composition of the passive layer with t_a. This possibility can be envisaged through the careful analysis of voltammetric changes.

The first anodic linear potential scan in the buffer solution shows up two peaks in the transpassive region, whereas only one peak appears in the stabilized voltammogram. This voltammetric response can be related to the presence of two kinds of Cr(III) species in the anodic layer after anodization of the 316SS specimen in the passive range. This Cr-species can be assigned to an outer Cr(III) containing a layer (layer II) which undergoes electrooxidation to soluble CrO_4^{2-} (peak AIII'). This interpretation is consistent with the absence of the corresponding conjugated cathodic peak for AIII', at least in the potential range covered by the experiments. Then, as t_a increases this Cr(III) species should become more strongly bound so that its electrooxidation should be progressively hindered. This explanation is consistent with the shift in the potential peak AIII' more positively as t_a increases. This implies a change in composition of layer II taking place during anodization leading to the formation of a stable chromium–oxygen–iron(II) compound where the iron constituent behaves as a non-reducible species, at least in the potential range of the thermodynamic stability of bulk water. This explanation is in agreement with the fact that the threshold potential of the HER shifts negatively as $E_{s,a}$ moves in the opposite direction.

The second kind of Cr(III) species (layer I) belonging to the inner part of the passivating layer originates in the chromium oxide layer already preexisting on the 316SS surface[3, 6]. According to the experimental results one can conclude that layer I is much less affected by the anodization time than the outer layer. Otherwise, when the potential is stepped to 0.6 V, the Cr(III) species at layer I can be electrooxidized to a Cr(VI) species (peak AIII) remaining in the passive layer, which can be electroreduced to Cr(III) in the potential range of peak CIII. This conclusion is firmly supported by ESCA results of preanodized 316SS specimens which furnish direct evidence of the inner Cr(III)-rich oxide layer and the outer Fe-rich Cr(III) oxide layer[14]. In this case for $t_a = 90$ s Fe(II) and Fe(III) can be detected in the outer layer, whereas for $t_a = 3600$ s, a comparatively large amount of Fe(II) is present in the layer, while that of Fe(III) tends to decrease. These data indicate that on increasing the polarization time an oxide layer with a chromite

structure is progressively formed at the outer layer[6]. On the basis of these results the different reaction pathways for the Cr(III) and Fe(II) electrooxidation reaction at the outer layer can be advanced for the corresponding optimal potential windows. Thus, for $E_s = -0.1$ V the reactions at the outer layer can be written as follows:

$$\text{Cr (Fe-containing alloy)} \overset{k_1}{\rightleftharpoons} \text{Cr(III)hydroxide(Fe-containing alloy)}, \quad (2)$$

$$\text{Cr(III)hydroxide(Fe-containing alloy)} \overset{k_2}{\rightarrow} \text{Fe chromite structure}, \quad (3)$$

and:

$$\text{Fe(in the alloy)} = \text{Fe(II)} + \text{Fe(III) hydrous oxide}, \quad (4)$$

where $k_1 \gg k_2$ denote the rate constants of the consecutive processes. Accordingly, Reaction (2) can be followed at short times, whereas Reaction (3) occurs after prolonged anodization times. On the other hand, for $E_s = 0.6$ V, the reactions at the outer layer can be described as follows:

$$\text{Cr(III) hydroxide (in the passive layer)} = \text{CrO}_4^{2-} \text{ (soluble)}, \quad (5)$$

and:

$$\text{Fe chromite structure} = \text{Cr(VI)} \text{ species in the passive layer}. \quad (6)$$

Reactions (2) to (6) describe the remarkable changes operating in the passive layer structure and composition and corresponding changes in the protective properties of the passive layer for localized attack by the aggressive anions.

Let us now discuss pit formation on passivated 316SS specimens. Localized corrosion of metals was interpreted through nucleation and kinetic growth laws[8, 10], particularly to describe the initiation of pitting. Nucleation and growth of new phases can approach two limiting conditions, depending on whether nucleation behaves as an irreversible or as a reversible process[15]. In the former case all sites (N_0) are converted into stable nuclei at the rate, $\alpha(t)$, and the converted sites remain covered by the nuclei in the course of the reaction. Otherwise, under reversible conditions the active sites can be converted into nuclei at the rate $\alpha(t)$, but incipient nuclei can also die out at the rate $\mu(t)$, so that certain nuclei sites become again active for new nucleation events in the time scale of the measurements. In this case unstable etch pits (current bursts) can be taken as typical for reversible nucleation. Otherwise, the rate of stable pit generation $\lambda(t)$, as an example of irreversible nucleation, is given by[16]:

$$\lambda(t) = aN_0\alpha(t), \quad (7)$$

where a (cm^2) is the electrode area and N_0 (cm^{-2}) is the number of sites available for nucleation. The nucleation rate $\alpha(t)$ is expressed in s^{-1}.

For a stationary nucleation rate, the probability of formation of at least one stable pit, $P_{n\geq 1}$, is given by[17, 18]:

$$P_{n\geq 1} = 1 - \exp(-\lambda t). \quad (8)$$

According to the Poisson distribution, Equation (8), the slope of the $\ln(1 - P_{n\geq 1})$ *vs* t plots yields the value of λ. When this approach is applied to the kinetic data obtained for 316SS in the buffer solution +0.5 M NaCl (Fig. 10) one can obtain a value of λ, (λ_1), the short time range *ie* $t < 16$ s. Likewise, for $t > 16$ s one can observe a clear deviation of the experimental data from the straightline plot which is presumably associated with a second value of λ, (λ_2). The latter, however, cannot be determined with reasonable accuracy from the present data. Nevertheless, if should be noticed that a multiplicity of λ values is not surprising as it has already been reported in previous works[10, 19] for the same alloy in aggressive media others than the one employed in the present case.

It is generally accepted that the value of λ depends on the applied potential, E_s,[19] although no consistent number of atoms in the critical nucleus could be obtained from the $\ln\lambda$ *vs* $(1/\eta)$ or $\ln\lambda$ *vs* η ($\eta = E_s - E_b$) plots[10]. This drawback can be overcome if the rate of pit generation can be related to the time required for the appearance of a breakdown site. It is this time rather than the formation time of a critical nucleus may be conceived either as the penetration time of a salt nucleus or the time for the local removal of the passive layer. Accordingly, the results obtained at a constant potential E_s, reveal the strong dependence of λ on the passive layer properties. Thus, for $E_a = -0.1$ V, the increase in t_a from 90 to 1800 s decreases λ from 1.1 to 0.055 s^{-1} (Fig. 10). Simultaneously, the value of $\langle n \rangle$ decreases considerably as t_a increases. This dependence of λ on t_a cannot be directly expected from simple acidification theories[20, 21] as previously suggested[8]. However, the fact that this dependence comes from runs where the passive layer thickness is only slightly changed indicates that the passive layer composition should be considered as the most relevant parameter for controlling the appearance of breakdown sites, instead of the passive layer thickness[22].

The reactions leading to the most protective passive layer should also explain the decrease of λ on decreasing either N_0 or α, or both simultaneously. For 316SS, the value of N_0 can be related to the surface density of sulphide inclusions in the metal, as revealed through EDAX. As previously suggested, sulphide inclusions should act as preferred sites for nucleation[10] changing the properties of the passive layer[4], and providing suitable paths for pit growth. However, only a

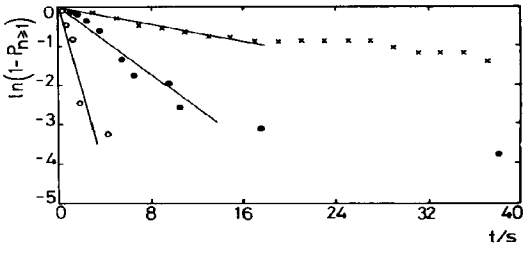

Fig. 10. $\ln(1 - P_{n-1})$ *vs* t plots: t_a = (o) 90; (•) 900; (x) 1800 s.

fraction of the sulphide inclusions participate in the pitting process as its total number lies in the 3000–5000 cm^{-2} range. As these values are exceedingly greater than the values of $\langle n \rangle$, the number of inclusions which are actually effective for pitting nucleation should be considered as a function of the passive layer structure. In this sense the increase in the prepassivation time favours the formation of the most protective layer structure leading to either a reduction of the number of inclusions available for pitting or increasing the time for passive layer removal or penetration by chloride ions, which lead to a decrease in the value of α.

It should be noted that the preceding discussion has been based upon data obtained at the same E_s values. Nevertheless, when E_s is shifted in the positive direction the passive layer properties can also be modified in the way of producing a loss of chromium and water[10]. This leads to a decrease in the repair ability of the protective layer and simultaneously in the stability of sulphide inclusions[23]. These effects result in the increase of either N_0 or α, or both simultaneously, and consequently, in the values of λ and $\langle n \rangle$ as previously reported[10].

Despite that on the basis of the data presented in this work the interpretation and discussion of results was principally based on the presence of Cr and S in the 316SS, the influence of other alloy components, principally Mo, on the entire process can not be disregarded. This matter will be discussed on a forthcoming publication where a comparative study of 316SS and 304SS will be presented.

Acknowledgements—This work was financially supported by the Consejo Nacional de Investigaciones Cientificas y Técnicas and the Comisión de Investigaciones Científicas de la Provincia de Buenos Aires. The authors wish to thank Majdalani S. A. for the supply of the stainless steel material used in the present work.

REFERENCES

1. Janik Czachor, *Werkst. Korros.*, 606 (1980).
2. H. J. Yearian, W. D. Derbyshire and J. F. Radavich, *Corrosion* **13**, 65 (1957).
3. N. Ramasubramian, N. P. Preocanin and R. D. Davison, *J. electrochem. Soc.* **132**, 793 (1985).
4. N. de Cristofaro, C. A. Acosta, R. C. Salvarezza and H. A. Videla, *Corrosion* **42**, 240 (1986).
5. S. C. Tjong, R. W. Hoffman and E. B. Yeager, *J. electrochem. Soc.* **129**, 1662 (1982).
6. J. C. Langevoort, I. Sutherland, L. J. Hanekamp and P. J. Gellings, *Appl. Surf. Sci.* **28**, 167 (1987).
7. M. Keddam, M. Krarti and C. Pallotta, *Corrosion* **43**, 454 (1987).
8. D. E. Williams, C. Westcott and M. Fleischmann, *J. electrochem. Soc.* **132**, 1796 (1985).
9. T. Shibata and T. Gakayama, *Corrosion* **33**, 243 (1977).
10. R. C. Salvarezza, N. De Cristofaro, C. Pallotta and A. J. Arvia, *Electrochim. Acta* **32**, 1049 (1987).
11. C. Pallotta, N. De Cristofaro, R. C. Salvarezza and A. J. Arvia, *Electrochim. Acta* **31**, 1265 (1986).
12. I. Olefjord, B. Broz and U. Jelvestam, *J. electrochem. Soc.* **132**, 2855 (1985).
13. I. Olefjord and B. Brox, in *Passivity of Metals and Semiconductors* (Edited by M. Froment), p. 561, Elsevier, Amsterdam (1983).
14. C. Pallotta, M. Urretabizkaya, N. De Cristofaro, R. C. Salvarezza and A. J. Arvia (in preparation).
15. S. Fletcher, *J. electroanal. Chem.* **215**, 1 (1986).
16. M. Abyaneh, M. Fleischmann and M. Labran, in *Proceedings of the Symposium on Electrocrystallization* (Edited by R. Weil and R. G. Barradas), Vol. 81-6, The Electrochemical Society, Pennington, New Jersey (1981).
17. R. Sridharan and R. de Levie, *J. electroanal. Chem.* **169**, 59 (1985).
18. A. Milchev and V. Tsakova, *Electrochim. Acta* **30**, 133 (1985).
19. N. Sato, *J. electrochem. Soc.* **129**, 261 (1982).
20. J. R. Galvele, *J. electrochem. Soc.* **129**, 464 (1976).
21. R. Galvele, *Corros. Sci.* **21**, 551 (1981).
22. T. Okada, *J. electrochem. Soc.* **131**, 241 (1984).
23. G. S. Elklund, *J. electrochem. Soc.* **123**, 170 (1976).